

Scanning Tunneling Microscopy Study of InAs epitaxy on GaAs(001)

S. Varma ^a, V. Bressler-Hill ^{b,c}, A. Lorke ^d, P. M. Petroff ^{b,d}
and W. H. Weinberg ^{b,c}

^a Institute of Physics, Bhubaneswar, 751005, India.

^b Center for Quantized Electronic Structures, University of California,
Santa Barbara, CA 93105, USA.

^c Chemical Engineering Department, University of California,
Santa Barbara, CA 93106, USA.

^d Materials Department, University of California, Santa Barbara, CA 93106,
USA.

Initial stages of InAs epitaxy on molecular beam epitaxy (MBE) -grown vicinal GaAs (001) surfaces have been studied using an ultrahigh-vacuum scanning tunneling microscope (STM). The growth of InAs islands is anisotropic leading to elongated islands with constrained growth along [110] direction. STM images reveal different growth mechanisms for the surfaces misoriented towards the [110] direction (A type) and the $\bar{1}\bar{1}0$ direction (B type). With increasing coverage, the anisotropy and density of the islands increases on the terraces. However, the size distribution of the islands in the [110] direction is narrow and independent of coverage, indicating that there is a preferred island width. Scaling properties associated with island size and separation distribution for these InAs islands are presented. Growth being anisotropic, island size distribution was separately studied along [110] and $\bar{1}\bar{1}0$ directions. Scaling is then only observed in the $\bar{1}\bar{1}0$ direction. Scaled radial distribution function of the islands shows clustering. We suggest that strain effects are limiting the island size in the [110] direction and are also causing the observed clustering in the radial distribution function.

Key Words : Heteroepitaxy, Strain, Scaling

PACS Nos. : 61.16.Ch, 68.60.Bs, 68.65.+g

I. Introduction

Studies of early stages of nucleation and growth have acquired large interest recently [1-8]. This has become possible due to techniques like STM with which one can study the growth at submonolayer coverages. The controlled growth

of nanostructures by MBE and their characterization by STM has resulted in the study of quantum structures with interesting properties. Recently, it was demonstrated that deposition of modest amounts of InAs on GaAs results in the formation of coherently strained InAs clusters or elongated islands which exhibit novel optical and transport properties [1-3]. These new properties are thought to be the result of two- and three-dimensional carrier confinement in the InAs within the GaAs matrix. Moreover, this is an excellent system for studying the effects of strain on the atomic structure (7% lattice mismatch).

There has been also much recent interest in employing scaling theories to describe nonlinear systems such as the initial stages of epitaxial growth [4], especially in the aggregation regime. Under these circumstances film growth is completely characterized by the development of the island size, shape, and separation distributions. A scaling theory has been reported for homoepitaxy in the aggregation regime which delineates the scaling properties of the island size and separation distributions at different temperatures and coverages [4]. In this theory the island size distribution, N_s , can be expressed as

$$N_s \sim [\theta/\langle s \rangle^2] f(s/\langle s \rangle) , \quad (1)$$

where N_s is the number of islands which contain s atoms normalized by the number of lattice sites, θ is the fractional surface coverage, $\langle s \rangle$ is the average number of atoms in an island, and $f(s/\langle s \rangle)$ is the scaling function. This scaling *ansatz* assumes that $f(s/\langle s \rangle)$ is independent of coverage and temperature in the aggregation regime [4]. Two-dimensional (2D) island scaling, based on this theory, was observed recently in STM images of Fe homoepitaxy [5].

Another scaling function that is of interest is the radial distribution function. For large diffusion rates the scaling relation for the island separation, $N(r)$, which is proportional to the probability of finding an island center separated by a distance, r , from the center of another island, is given by [4]

$$N(r) \sim N g(r/\langle R \rangle) , \quad (2)$$

where N is the macroscopic number density of islands, and $\langle R \rangle \sim 1/\sqrt{N}$ is a measure of the average separation between island centers if they are uniformly separated [4]. The scaling function (the radial distribution function), $g(r/\langle R \rangle)$, has the property that $g(r/\langle R \rangle) \rightarrow 0$ for $r \rightarrow r_0$ and $g(r/\langle R \rangle) \rightarrow 1$ for $r \rightarrow \infty$ where r_0 is the average size of an individual island. Since this distribution is determined by the distribution of nucleation sites, anisotropies in a noninteracting system will not affect it.

It would be useful to determine whether these scaling *ansatz* also characterize the initial *heteroepitaxial growth* of semiconductors. These systems are

inherently more complex due both to their covalent bonding and to diffusion, reaction, and reconstruction anisotropies that dominate the growth morphologies.

Using an ultrahigh vacuum (UHV) STM, we have studied MBE-grown GaAs on vicinal (001)-(2x4) surfaces with submonolayer coverages of InAs. We have investigated surfaces misoriented towards the [110] direction (A-type) and the $\bar{[110]}$ direction (B-type), and we observe that the preferred InAs nucleation sites are different for the two orientations. In addition, regardless of coverage ($\theta = 0.15, 0.29, 0.35$) or surface misorientation, InAs islands are observed which have a preferred width in the [110] direction. We suggest that strain effects are limiting the island size in the [110] direction.

Recent theoretical work by Ratsch and Zangwill [6] has suggested that the principal effect of strain during growth is to reduce the energy barrier to adatom detachment from an island, and they have shown with MC simulations that 2D island growth in strained, isotropic, heteroepitaxial systems can also be characterized by the scaling relations, Eq. (1) and Eq. (2).

The scaling properties associated with the island size and separation distributions for different coverages for InAs growth on GaAs(001)-(2x4) are presented here. The island size distribution obeys scaling when considering the average total island size. However, considering the anisotropy of the observed island shapes, when the average size of the island is separated into its [110] and $\bar{[110]}$ components, the scaling is then only observed in the $\bar{[110]}$ direction and not in the [110] direction. Furthermore, an analysis of the radial distribution of islands indicates that the islands are not distributed uniformly. Both of these important observations are a consequence of the strain which is present in this lattice-mismatched system.

II. Experimental Procedures

Two vicinal GaAs substrates misoriented by $1 \pm 0.1^\circ$ towards the [110] and $\bar{[110]}$ azimuths, respectively, were used in the investigation. After the removal of oxide at 630°C , a 500 nm GaAs buffer layer was grown at 600°C on both the substrates. After this, a 120 nm thick tilted superlattice (TSL) was grown by depositing alternating layers of 0.5 ML GaAs and 0.5 ML AlAs under the same growth conditions as for the GaAs buffer layer. A 4 ML cap of GaAs was then deposited to regain a stoichiometric GaAs(001)-(2x4) surface. This growth sequence has proved to result in periodic step structures and well-ordered (2x4) reconstructed terraces. The TSL layer was not grown on the B-type surfaces since there is no evidence for step bunching on this surface. The samples were Si-doped ($N_d = 1 \times 10^{18} \text{ cm}^{-3}$). The growth conditions used were the same

as in ref. [7]. All samples were quenched to room temperature by decreasing both the substrate temperature and the As pressure. The RHEED pattern remained (2x4) at room temperature. A control sample was removed from the growth stage, and the remaining samples were returned to the growth chamber for InAs deposition. The samples were carefully heated to 450 °C under low As background pressure to maintain the (2x4) reconstruction, and fractional coverages ($\theta = 0.15$ and 0.35) of InAs were deposited. Samples with InAs deposition (of $\theta = 0.29$) on flat GaAs substrates were also studied. During InAs deposition the RHEED pattern in the [110] azimuth was monitored to provide us the estimate of InAs coverage. Using an ion-pumped interlock shuttle all samples were then transferred from the MBE system to the STM chamber. All of the STM images which are shown were measured at a tunneling current of 0.1 nA and a sample bias of -2.4 to -3.5 V using platinum-iridium tips.

III. Results and Discussion

A. InAs Deposition on A-type Surfaces

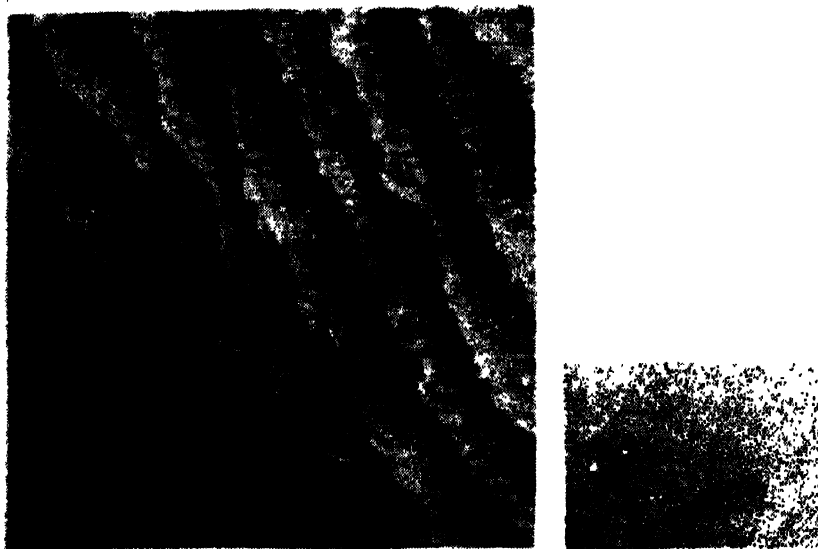


Fig. 1: A 200 x 200 nm² STM image of a clean 1⁰A-type GaAs(001)-(2x4) surface.

Fig. 1 shows a STM image of a clean 1⁰A-type GaAs(001)-(2x4) surface. The steps are regularly spaced, and the average terrace width on this surface was calculated to be 240 Å indicating a local misorientation of 0.75°.

A high-resolution STM image of the GaAs surface after a deposition of 0.35 ML of InAs is shown in Fig. 2. The step edges are uniformly spaced. The GaAs (2x4) reconstruction is still observed. We now also observe some

areas of surface which appear different than the surrounding reconstruction. We conclude that these patches or islands are composed of InAs since the coverage of these islands determined from the STM images agrees with the deposited InAs coverage (calibrated using RHEED oscillations).

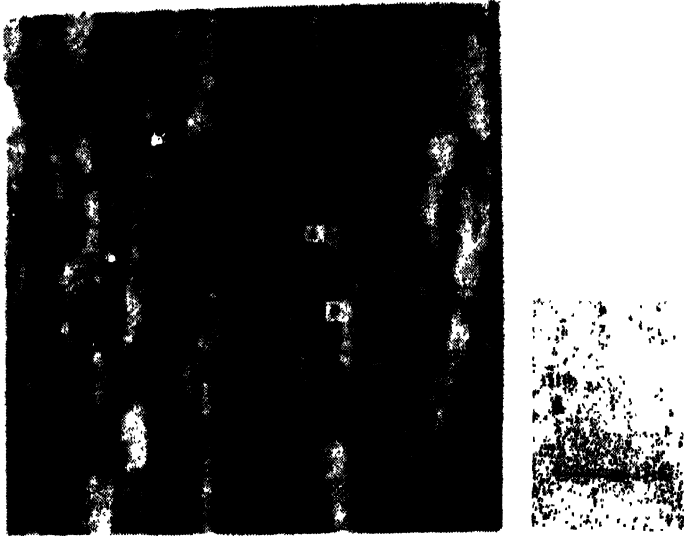


Fig. 2: A 100 x 100 nm² STM image of the 1° A-type GaAs(001)-(2x4) surface with an InAs coverage of $\theta = 0.35$. For clarification, the step edges have been outlined in black. Note the anisotropy of the InAs islands. Some islands exhibit separate domains of indium and arsenic termination. An In-terminated domain (A) and an As-terminated domain (B) are indicated with arrows [7].

The existence of islands shows that In is mobile on the surface at this deposition temperature (450 °C). InAs is predominantly forming islands on the terrace. At this coverage the InAs-related structure is also observed on some of the step edges. The growth on the terraces, though, is 2.5 times more likely than at the step edge indicating that the step edge is not the preferred nucleation site at this temperature. Most of the patches of InAs, whether island, step, or defect related, are ordered. From the detailed line scans we have determined that the In-terminated patches are c(4x4) reconstructed [7]. At this coverage, the InAs islands are quite elongated in the $[1\bar{1}0]$ direction. Interestingly, all the islands studied possessed a characteristic width of ~ 4 nm along the $[110]$ direction. These islands are predominantly two-dimensional, although some second-layer growth is observed.

At $\theta = 0.15$ and 0.29 , though the InAs islands on GaAs substrates were less anisotropic than islands at $\theta = 0.35$, they were still constrained in the $[110]$ direction [7, 8]. Surprisingly, there is little or no change in the island size

in the $[110]$ direction with increasing coverage. The mean island size in this direction was determined to be 4.0 ± 1.0 nm for all the coverages ($\theta = 0.15, 0.29, 0.35$). However, significant growth in the $[\bar{1}10]$ direction occurred with the average island size increasing from 7.7 ± 3.9 nm at $\theta = 0.15$ to 19.3 ± 11.5 nm and $\theta = 0.35$. The large standard deviations reflect the existence of variable island-sizes in this direction. The island size distributions and their scaling functions will be discussed in sec. III C.

B. InAs Deposition on B-type Surfaces

A high-resolution image of InAs on the B-type GaAs(001)-(2x4) surface with a coverage of $\theta = 0.35$ is shown in Fig. 3. The B-type surface has step edges which are irregular, and many defects are observed on the terraces such as missing rows of the (2x4) unit cell.



Fig. 3: A high-resolution 100×60 nm² STM image of 0.35 ML of InAs on the 1st B-type GaAs(001)-(2x4) surface. The step edges have been outlined in black.

Areas of the GaAs(001)-(2x4) reconstruction are clearly visible in Fig. 3. The local InAs structure is resolved in the terrace vacancies and at the step edges. Compared to the A-type surface, there is more growth at step edges on this surface. This is not surprising considering the anisotropy of the islands observed on the A-type surface which suggests that the diffusion of In in the $[\bar{1}10]$ direction on GaAs(001) is faster than diffusion in the $[110]$ direction.

The anisotropy of the islands for B-type surface increases with increasing terrace width. This indicates that the width of the terrace (barrier at the step edge) is limiting growth in the $[\bar{1}10]$ direction. However, the size of the islands in the $[110]$ direction remains constant (within ± 1 nm) irrespective of

the terrace width. Furthermore, it is the same size that is observed on the A-type step (i.e. 4 ± 1.0 nm).

We conjecture that the edges of the islands along the $[\bar{1}10]$ direction for both A -type and B type surfaces are relaxing to accommodate the strain and that 4 ± 1 nm (in the $[110]$ direction) is the preferred size for this relaxation. Support for the existence of a preferred island size for submonolayer coverages comes from in situ RHEED measurements [9].

Moreover, the InAs islands are not isotropic. There is considerable growth and non-uniformity of the islands in the $[\bar{1}10]$ direction. The fact that growth seems not to be limited in the $[\bar{1}10]$ direction indicates that most of the strain is accommodated by elastic deformation along the $[110]$ direction. In addition, the $c(4 \times 4)$ reconstruction of the InAs may be reducing strain in this direction.

C. Scaling Studies: Size Distribution

The island size distribution, N_s , considering the total number of atoms in an island, s , is shown in the inset of Fig. 4(a) (for $\theta = 0.15, 0.29, 0.35$). The distributions broaden as the fractional coverage of InAs increases, and they are similar to island size distributions observed both experimentally for homoepitaxy of Fe [5] and in MC simulations of unstrained systems [4]. This is a surprising result considering the significant strain which is present in our system.

To clarify the effect of strain on the growth of InAs, we have evaluated the linear island size distribution along the two orthogonal step-edge directions. The insets to Fig. 4(b) and 4(c) show N_s as a function of the linear number of atoms in an island along the $[110]$ direction, $s_{[110]}$, and along the $[\bar{1}10]$ direction $s_{[\bar{1}10]}$, respectively. The island size distribution in the $[110]$ direction shows distinctly different behavior from the $[\bar{1}10]$ direction.

Since the $[\bar{1}10]$ distribution is qualitatively similar to the distribution of total atoms in an island, the growth behaves as if it is unstrained in the $[\bar{1}10]$ direction; whereas growth in the $[110]$ direction is *quenched* by strain. As seen in Fig. 4, the most probable growth in the $[110]$ direction is for $s = 9 \pm 1$ atoms. This corresponds to an island width of ~ 4 nm, the characteristic width observed along this direction irrespective of the coverage or the surface misorientation.

The scaling properties of the three distributions are also shown in Fig. 4. As suggested by Eq. (1), the quantity $\langle x \rangle^2 N_s / \theta$ is plotted as a function of $s / \langle x \rangle$, with the metric of the average island size taken to be $\langle x \rangle = \langle s \rangle$, $\langle s_{[110]} \rangle$, and $\langle s_{[\bar{1}10]} \rangle$ in Fig. 4(a), 4(b), and 4(c), respectively.

Collapse of the data onto a single curve is observed for $\langle x \rangle = \langle s \rangle$ in Fig.

4(a), indicating that scaling is obeyed in this case and demonstrating that the scaling theory characterizing homoepitaxy can be applied to strained heteroepitaxy as well.

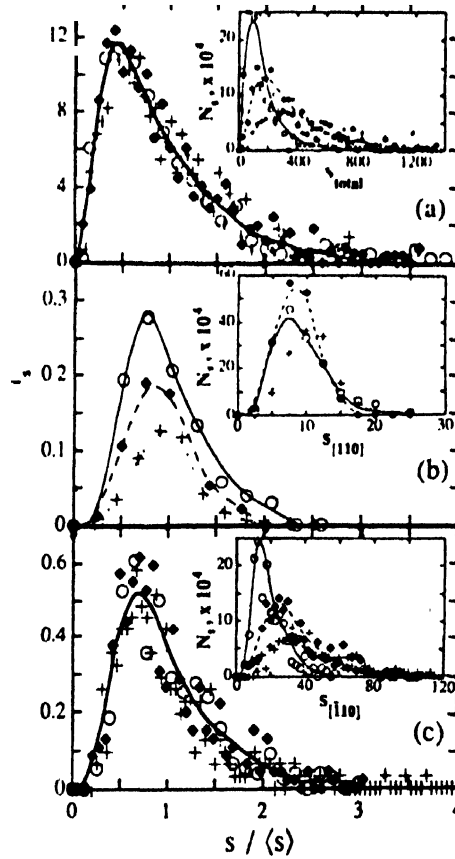


Fig. 4: $\langle x \rangle^2 N_s / \theta$ is plotted as a function of $s / \langle x \rangle$, with $\langle x \rangle = \langle s \rangle$, $\langle s_{[110]} \rangle$, and $\langle s_{[\bar{1}10]} \rangle$ in (a), (b), and (c), respectively. The lines are a smooth fit to the data. The insets show the corresponding size distribution for each scaling relation, as described in the text.

The effect of strain on the scaling is only apparent when the distributions describing the islands in the $[\bar{1}10]$ and $[110]$ direction are plotted separately. Collapse of the data is observed for $\langle x \rangle = \langle s_{[\bar{1}10]} \rangle$, indicating that the growth behaves as if it is unstrained in this direction, cf., Fig. 4(c); when $\langle s_{[110]} \rangle^2 N_s / \theta$ is plotted as a function of $s / \langle s_{[110]} \rangle$, however, scaling is not obeyed as may be seen clearly in Fig. 4(b).

The strain, we suggest, is limiting the growth in the $[110]$ direction. It also results in scaling distribution functions that do not scale in the direction where InAs islands are constrained.

D. Scaling Studies: Radial Distribution

The scaled radial distribution functions $Ng(r/\langle R \rangle)$ of Eq. (2) are shown in Fig. 5 (for $\theta = 0.15, 0.29, 0.35$). Collapse of the distribution onto a single curve is observed for all three coverages.

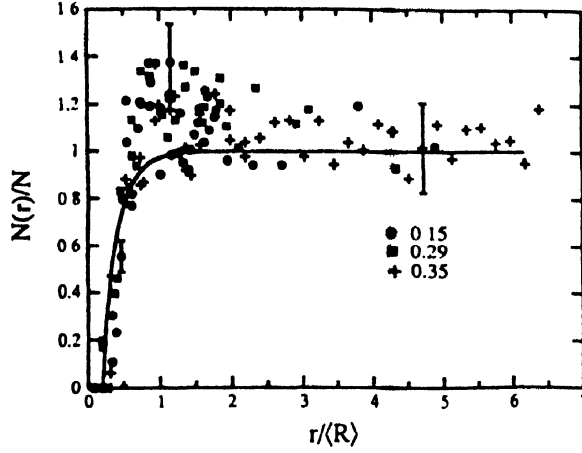


Fig. 5: Scaled radial distribution function for finding an island separated by a distance r from a given island. The solid line is given by $\left\{1 - K_0(r/\sqrt{D\tau})/K_0(r_0/\sqrt{D\tau})\right\}$, where K_0 is the modified Bessel function of order zero, and $D\tau \sim 1/4\pi N$ with $\sqrt{N} \sim 1/\langle R \rangle$ [4]. The parameter $r_0/\langle R \rangle = 0.2$. The error bars denote the standard error in the measurement.

The depletion of islands at small separations, $r_0 \lesssim r \lesssim \langle R \rangle/2$, is due to the low nucleation probability in the vicinity of an existing island, which acts as a trap for diffusing adatoms. A through-substrate strain-induced repulsion is also expected to result in a lower probability of island nucleation in this region.

The clustering of islands at $r \gtrsim \langle R \rangle$ suggests an increased adatom density in this region. This is a consequence of the strain which is present along the $[110]$ direction: the $\overline{[110]}$ edge acts as a sink for adatoms, while the $[110]$ edge, due to the strain-limited growth, is not nearly so reactive. Adatoms undergoing detachment as a result of strain along the $[110]$ direction are available for nucleation if they encounter another adatom. This clustering was not observed for homoepitaxy [5] and hence can be used to quantify strain in the system.

IV. Conclusions

In summary, we have studied MBE-grown vicinal GaAs(001)-(2x4) surfaces after sub-monolayer deposition of InAs at 450 °C. The growth of InAs on A

type GaAs at this temperature proceeds by two-dimensional nucleation on the terrace vacancies. On B-type surfaces, on the other hand, InAs nucleates predominantly, but not exclusively, at the step edges and in the vacancies on the terraces. Regardless of coverage or surface misorientation, InAs islands are observed to have a preferred width of 4 nm in the $[110]$ direction. We conjecture that strain effects are limiting the island size in the $[110]$ direction.

We have also shown that the scaling theory developed for homoepitaxy may also be applied to strained heteroepitaxy. However if the size distribution in the two anisotropic directions is separated then the scaling is only observed in the $[\bar{1}10]$ direction and not in the $[110]$ direction. Strain is also responsible for the existence of an increased density of islands at separations $r \gtrsim \langle R \rangle$ in the radial distribution function.

References

- [1] D. Leonard, M. Krishnamurthy, C. M. Reaves, S. P. Denbarars, and P. M. Petroff, *Appl. Phys. Lett.* **63**, 3203 (1993)
- [2] O. Brandt, L. Tapfer, K. Ploog, R. Bierwolf, M. Hohenstein, F. Phillipp, H. Lage, and A. Heberle, *Phys. Rev.* **B44**, 8043 (1991).
- [3] A. Lorke, T. Noda, Y. Nagmune, Y. Nakamura, H. Sugawara, and H. Sakaki, in *Proceedings of the 21st Int. Conf. on the Physics of Semiconductors, China*, (1992) p. 1258.
- [4] M. C. Bartelt and J. W. Evans, *Phys. Rev.* **B46**, 12675 (1992); J. W. Evans and M. C. Bartelt, *Surf. Sci.* **284**, L437 (1993); and M. C. Bartelt, M. C. Tringides, and J.W. Evans, *Phys. Rev.* **B47**, 13891 (1993).
- [5] J. A. Stroscio and D. T. Pierce, *Phys. Rev.* **B49**, 8522 (1994).
- [6] C. Ratsch and A. Zangwill, *Appl. Phys. Lett.* **63**, 2348 (1993).
- [7] V.B. Hill, A. Lorke, S. Varma, P.M. Petroff, K.Pond and W.H. Weinberg, *Phys. Rev. B.* **50**(1994) 8479.
- [8] V.B. Hill, S. Varma, A. Lorke, B.Z. Nosho, P.M. Petroff, and W.H. Weinberg, *Phys. Rev. Lett.* **74**(1995) 3209.
- [9] J. Massies and N. Grandjean, *Phys. Rev. Lett.* **71**, 1411 (1993).